

## ***Electronic Supplementary Information***

### **Water-oxidation catalysis by synthetic manganese oxides – systematic variations of the calcium birnessite theme**

**Carolin Frey,<sup>a</sup> Mathias Wiechen,<sup>b,c</sup> and Philipp Kurz<sup>\*a</sup>**

<sup>a</sup> *Institut für Anorganische und Analytische Chemie, Albert-Ludwigs-Universität Freiburg, Albertstraße 21, 79104 Freiburg, Germany.*

*E-mail: philipp.kurz@ac.uni-freiburg.de; phone: +49 (0)761 203 6127.*

<sup>b</sup> *Institut für Anorganische Chemie, Christian-Albrechts-Universität zu Kiel, Max-Eyth-Str. 2, 24118 Kiel, Germany.*

<sup>c</sup> *current address: School of Chemistry, Monash University, Melbourne, 3800, Australia.*

## ***Physical and spectroscopic measurements***

### **Thermogravimetric analyses (TG)**

TG analyses were carried out by using a Netzsch STA 429. The samples were heated to 1000°C at a rate of 4 K min<sup>-1</sup> under a flow of air (75 mL min<sup>-1</sup>) in Al<sub>2</sub>O<sub>3</sub> crucibles. The TG data were corrected for buoyancy and current effects.

### **IR**

Infrared spectra of the solid compounds were measured on Bruker Alpha P (**Ca<sub>□</sub>** and **R<sub>y</sub>**) or Thermo Scientific Nicolet iS10 FT-IR (for oxides **T<sub>z</sub>**) spectrometers, both equipped with diamond ATR units.

### **X-ray powder diffractometry**

X-ray powder patterns for oxides **Ca<sub>□</sub>** and **R<sub>y</sub>** were measured in reflection geometry using a PANalytical X'Pert PRO instrument with Cu-K<sub>α</sub> radiation. For the products of the temperature series (oxides **T<sub>z</sub>**), a STOE STADI-P diffractometer was used. Here, the patterns were measured with Cu-K<sub>α</sub> radiation in transmission mode with ~20 mg of the oxide samples held by a polyacetate film in round sample holders (inner diameter ~15 mm).

### **BET analysis**

N<sub>2</sub> physisorption isotherms were measured with Microtrac BelsorpMINI (oxides **Ca<sub>□</sub>** and **R<sub>y</sub>**) or Porotec Sorptomatic 1990 instruments (oxides **T<sub>z</sub>**) and analysed according to the BET theory to determine the S<sub>BET</sub> surface areas listed in Table 1.

### **SEM**

SEM images of the oxides were taken using ZEISS ULTRA plus (**Ca<sub>□</sub>** and **R<sub>y</sub>** series) or LEO 1525 (**T<sub>z</sub>** series) scanning electron microscopes.

## Chemical analyses

### Ion chromatography (IC)

Ion contents of manganese, calcium and potassium were determined on a Metrohm 882 Compact IC plus ion chromatograph equipped with a Metrosep C4 150/4 column. A solution of dipicolinic acid (0.75 mM) and nitric acid (2 mM) served as IC eluent and the chromatograph was calibrated using AAS standard solutions obtained from Merck (for Mn) and Roth (K and Ca), respectively.

Prior to analysis ~10 mg of the oxide samples were treated with 1 mL of a mixture of concentrated HNO<sub>3</sub> and 30 % H<sub>2</sub>O<sub>2</sub> (1:10) to completely dissolve the oxide and to convert all manganese into its Mn<sup>2+</sup> form. The solutions were then diluted to 250 mL and 20 μL were injected into the IC system.

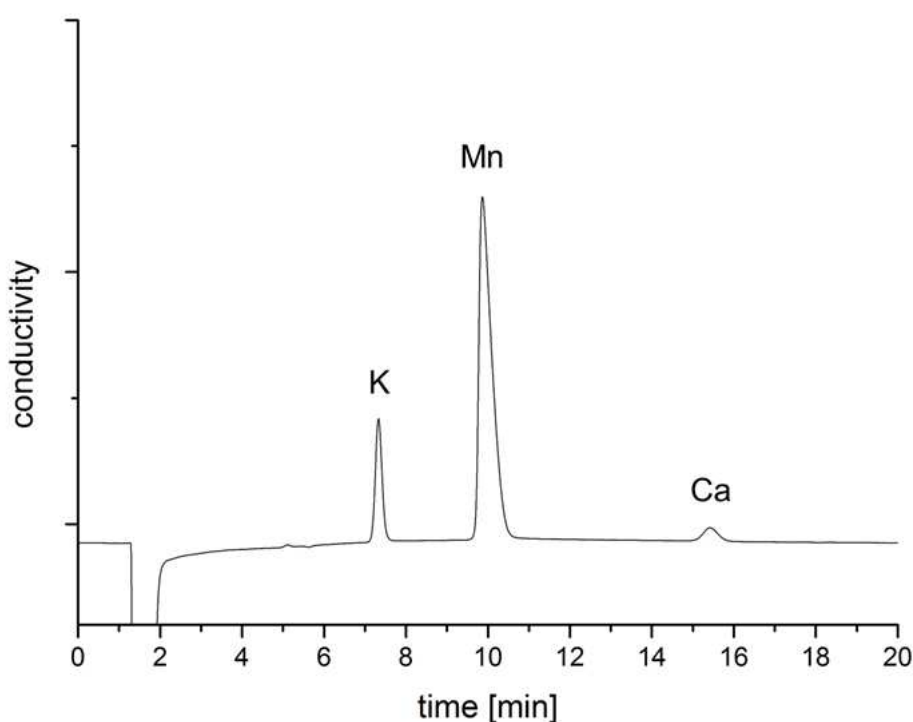


**Figure S1.** IC chromatogram for oxide Ca<sub>0.03</sub>, dissolved in a HNO<sub>3</sub> / H<sub>2</sub>O<sub>2</sub> mixture. The large negative peak detected between 1 and 2 min. is the injection peak originating from HNO<sub>3</sub> / H<sub>2</sub>O<sub>2</sub> in the solution.

### Determination of the average manganese oxidation state by redox titration

The method followed an established procedure for the quantification of MnO<sub>2</sub>.<sup>1</sup> Carefully weighed samples of the oxides (100-150 mg) were mixed with a solution of sodium oxalate (10 mL, 0.2 M) and sulphuric acid (10 mL, 0.5 M). The solution was stirred at 60°C until all oxide had dissolved. In this step manganese is quantitatively reduced to its Mn<sup>2+</sup> form. In the following, the excess of oxalate was determined by manganometric titration. In combination with the manganese content of the material (determined by IC, see above), the average oxidation state of the manganese centres could then be calculated.

## Catalytic measurements

### Oxygen detection by gas chromatography

To determine the concentration of oxygen in the headspace of the reaction vessels, gas chromatograms were recorded. For catalytic experiments on the calcium and ripening time series (oxides  $\text{Ca}_\square$  and  $\text{R}_y$ ), we used a HP 6890 Series GC System equipped with a 8 ft. x 1/8 in. 5 Å molsieve column (Supelco), for those concerning the oxides  $\text{T}_z$ , a PerkinElmer Clarus 480 with a 12 ft. x 1/8 in. 5 Å molsieve column (Restek) column. In all cases the carrier gas was helium, the GC oven temperature was set to 70 °C and  $\text{O}_2$  and  $\text{N}_2$  were quantified by a thermal conductivity detector (TCD). Figure S2 shows an example of a typical series of gas chromatograms measured for one catalytic run at 10 min intervals.

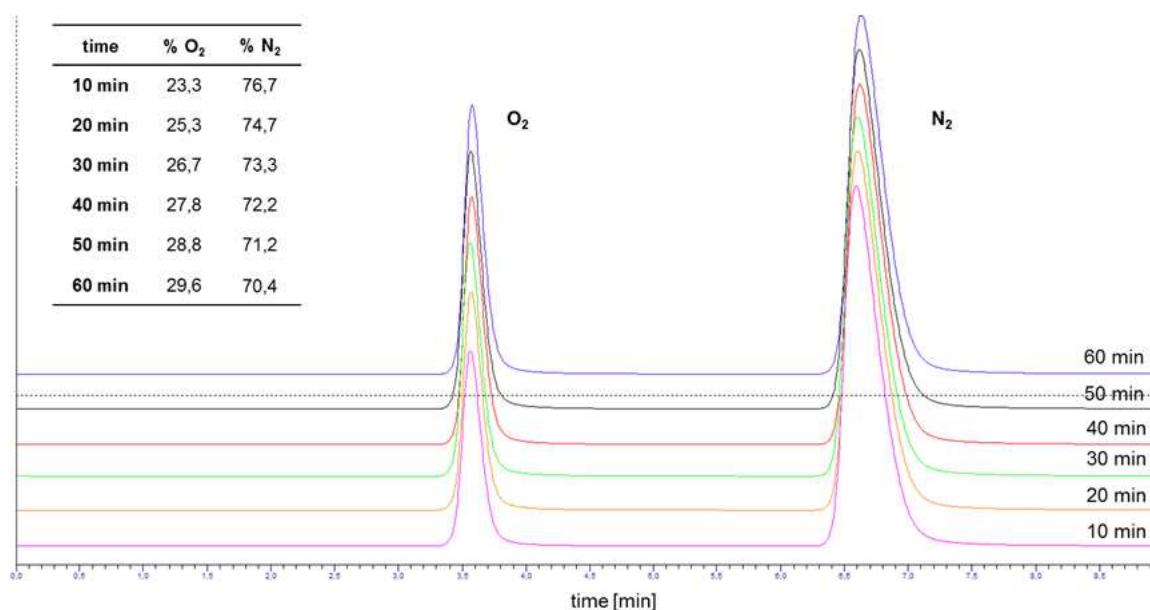


**Figure S2.** Series of GC traces for an experiment to determine WOC rates. Here, the traces for the reaction of the oxide  $\text{T}_{60}$  with  $\text{Ce}^{\text{IV}}$  are shown. The change in the relative areas of the  $\text{O}_2$  and  $\text{N}_2$  peaks, used for the calculation of the evolved oxygen, is listed in the inset table.

### Determination of water-oxidation catalysis rates for $\text{Ce}^{\text{IV}}$ -experiments

The method followed a previously developed procedure successfully employed before.<sup>2</sup> Precisely weighed oxide samples (about 5 mg) and 685 mg (1.25 mmol) of ammonium cerium(IV) nitrate,  $(\text{NH}_4)_2\text{Ce}(\text{NO}_3)_6$ , were filled into 20 mL septum vials. After the addition of 5 mL of air-saturated water, the vials were capped immediately using gas-tight septa and sonicated for 20 s.

For the series  $\text{Ca}_\square$  and  $\text{R}_y$ , headspace gas from the vials was injected into the GC using a HP 7694 headspace sampler equipped with a 1 mL sample-loop. Six headspace extractions out of a single septum vial were realised in intervals of 10 min. Therefore, the multiple headspace extraction value was set to 6, the vial equilibration time of the headspace sampler was set to 8.6 min, pressurize time to 0.10 min, loop fill time to 0.20 min, loop equilibration time to 0.10 min and the injection time to 1.0 min, giving an overall cycle time of 10 min and an overall time of 1 h for each measurement. The following temperature settings were used: temperature reaction vial : 40°C, sample loop temperature: 50°C, transfer line temperature: 65°C.

For reactions of the  $T_z$  series, the reaction containers were kept at 40°C in a water bath and headspace gas samples (100  $\mu$ l) were injected by hand using a gas tight syringe (Hamilton). As for the runs of  $Ca_{\square}$  and  $R_y$ , six injections at 10 min intervals were carried out.

The amount of oxygen evolved was then calculated for each headspace extraction from the detected  $O_2:N_2$  signal ratios. To do so, the amount of oxygen from air (corresponding to the detected nitrogen peak) was calculated and subtracted, leaving the excess  $O_2$  generated by the water-oxidation reaction.

In runs using auto-sampler injections, the pressurization of the septum vials before every single measurement has to be considered, which causes a dilution of the headspace with the helium carrier gas. In addition, leakage can occur after first puncture of the septa by the headspace sampler needle in multiple headspace extraction mode. Thus, the detected values for  $O_2$  and  $N_2$  were corrected by a factor calculated from repeating the experiments as described above, but with only one headspace extraction at the end of the interval of 1 h.

In all cases (auto-sampler and hand injection runs), the measurements to determine the catalytic rates reported in Table 1 were carried out at least two times for each oxide. If large differences between catalytic runs for the same oxide were observed, additional runs were performed. The values in Table 1 are the average rates from multiple runs, rounded to  $25 \text{ mmol}_{O_2} \cdot \text{mol}_{Mn} \cdot \text{h}^{-1}$ . Given the complex, multi-step procedure to obtain the catalytic rates, a mathematically precise error analysis is thus not possible. However, when we consider the observed differences in rates for multiple runs on identical oxides, we estimate the error margin for the rate determination to be in the range of  $\pm 10\%$ , which is the value indicated by error bars in Figure 7.

For a comparison of the detected oxygen evolution values, the rates have to be normalized. As manganese is the only redox active element here and redox processes have to occur during water oxidation catalysis, we decided to present oxygen evolution rates normalized to the amount of manganese and calculated them as  $\text{mmol } O_2$  per  $\text{mol Mn}$  and hour. Though this is done by other groups, too,<sup>2,3</sup> we are aware of the fact that other normalization methods, notably rates per  $S_{BET}$  surface,<sup>4</sup> have also been used. However, as discussed in detail before,<sup>2</sup> we are still of the opinion that rates per redox active metal centre are the most meaningful way of comparing rates for water-oxidation catalysis.

## Additional Tables and Figures

**Table S1.** Details concerning the variations of reaction parameters and chemical formulae for the studied synthetic oxides.

		<i>synthesis parameters</i>			
	oxide no.	amount <i>x</i> of Ca(AcO) <sub>2</sub> in solution B	buserite ripening time <i>y</i> [hours]	drying temperature <i>z</i> [°C]	Chemical formulae <sup>a</sup>
<i>calcium series</i>	Ca <sub>0.00</sub>	-	0	65	K <sub>0.31</sub> Ca <sub>0.00</sub> MnO <sub>2.00</sub> · 0.5 H <sub>2</sub> O
	Ca <sub>0.03</sub>	141 mg (0.8 mmol)	0	65	K <sub>0.28</sub> Ca <sub>0.03</sub> MnO <sub>2.02</sub> · 0.6 H <sub>2</sub> O
	Ca <sub>0.13</sub>	564 mg (3.2 mmol)	0	65	K <sub>0.42</sub> Ca <sub>0.13</sub> MnO <sub>2.24</sub> · 1.5 H <sub>2</sub> O
	Ca <sub>0.21</sub>	846 mg (4.8 mmol)	0	65	K <sub>0.20</sub> Ca <sub>0.21</sub> MnO <sub>2.21</sub> · 1.4 H <sub>2</sub> O
	Ca <sub>0.28</sub>	1.13 g (6.4 mmol)	0	65	K <sub>0.19</sub> Ca <sub>0.28</sub> MnO <sub>2.33</sub> · 1.9 H <sub>2</sub> O
	Ca <sub>0.36</sub>	1.41 g (8.0 mmol)	0	65	K <sub>0.09</sub> Ca <sub>0.36</sub> MnO <sub>2.30</sub> · 1.7 H <sub>2</sub> O
	Ca <sub>0.63</sub>	2.82 g (16 mmol)	0	65	K <sub>0.01</sub> Ca <sub>0.63</sub> MnO <sub>2.54</sub> · 2.0 H <sub>2</sub> O
<i>ripening time series</i>	R <sub>0h</sub>	1.13 g (6.40 mmol)	0	65	K <sub>0.03</sub> Ca <sub>0.28</sub> MnO <sub>2.25</sub> · 1.2 H <sub>2</sub> O
	R <sub>4h</sub>	1.13 g (6.40 mmol)	4	65	K <sub>0.06</sub> Ca <sub>0.28</sub> MnO <sub>2.21</sub> · 1.3 H <sub>2</sub> O
	R <sub>8h</sub>	1.13 g (6.40 mmol)	8	65	K <sub>0.15</sub> Ca <sub>0.29</sub> MnO <sub>2.26</sub> · 1.4 H <sub>2</sub> O
	R <sub>12h</sub>	1.13 g (6.40 mmol)	12	65	K <sub>0.38</sub> Ca <sub>0.27</sub> MnO <sub>2.31</sub> · 2.1 H <sub>2</sub> O
	R <sub>24h</sub>	1.13 g (6.40 mmol)	24	65	K <sub>0.15</sub> Ca <sub>0.27</sub> MnO <sub>2.25</sub> · 1.3 H <sub>2</sub> O
	R <sub>120h</sub>	1.13 g (6.40 mmol)	120	65	K <sub>0.07</sub> Ca <sub>0.28</sub> MnO <sub>2.27</sub> · 1.3 H <sub>2</sub> O
	R <sub>240h</sub>	1.13 g (6.40 mmol)	240	65	K <sub>0.03</sub> Ca <sub>0.28</sub> MnO <sub>2.25</sub> · 1.5 H <sub>2</sub> O
<i>temperature series</i>	T <sub>60</sub>	0.85 g (4.8 mmol)	2	60	K <sub>0.04</sub> Ca <sub>0.20</sub> MnO <sub>2.17</sub> · 1.2 H <sub>2</sub> O
	T <sub>200</sub>	0.85 g (4.8 mmol)	2	200	K <sub>0.05</sub> Ca <sub>0.21</sub> MnO <sub>2.18</sub> · 0.7 H <sub>2</sub> O
	T <sub>400</sub>	0.85 g (4.8 mmol)	2	400	K <sub>0.05</sub> Ca <sub>0.20</sub> MnO <sub>2.12</sub> · 0.3 H <sub>2</sub> O
	T <sub>600</sub>	0.85 g (4.8 mmol)	2	600	K <sub>0.04</sub> Ca <sub>0.20</sub> MnO <sub>2.02</sub> · 0.1 H <sub>2</sub> O
	T <sub>800</sub>	0.85 g (4.8 mmol)	2	800	K <sub>0.06</sub> Ca <sub>0.22</sub> MnO <sub>1.95</sub> · 0.0 H <sub>2</sub> O
	T <sub>1000</sub>	0.85 g (4.8 mmol)	2	1000	K <sub>0.00</sub> Ca <sub>0.22</sub> MnO <sub>1.62</sub> · 0.0 H <sub>2</sub> O

<sup>a</sup> The following *three-step procedure* was used to determine the chemical formulae of the synthetic oxides:

1. The K:Mn / Ca:Mn ratios determined by ion chromatography were set as stoichiometric indices  $K_a$  and  $Ca_b$ . As all elemental compositions were given relative to manganese  $Mn_c$  is set to 1.
2. The total cation charge per unit was calculated as **total charge** =  $a + 2b + Ox_{Mn}$ , where  $Ox_{Mn}$  is the average Mn oxidation state determined by redox titration. Assuming that all negatively charged ions are  $O^{2-}$ , the stoichiometric index  $O_c$  was set as  $c = \frac{1}{2}$  **total charge**.
3. Finally, and on the assumption that the only additional species present in the oxides are water molecules, the amount of water was adjusted in such a way that the Mn content determined by IC fits the formula. Of course, the listed scenario for the contents of  $O^{2-}$  and  $H_2O$  is just one possibility and any combination of  $O^{2-}$ ,  $OH^-$  and  $H_2O$  matching the dataset is possible.

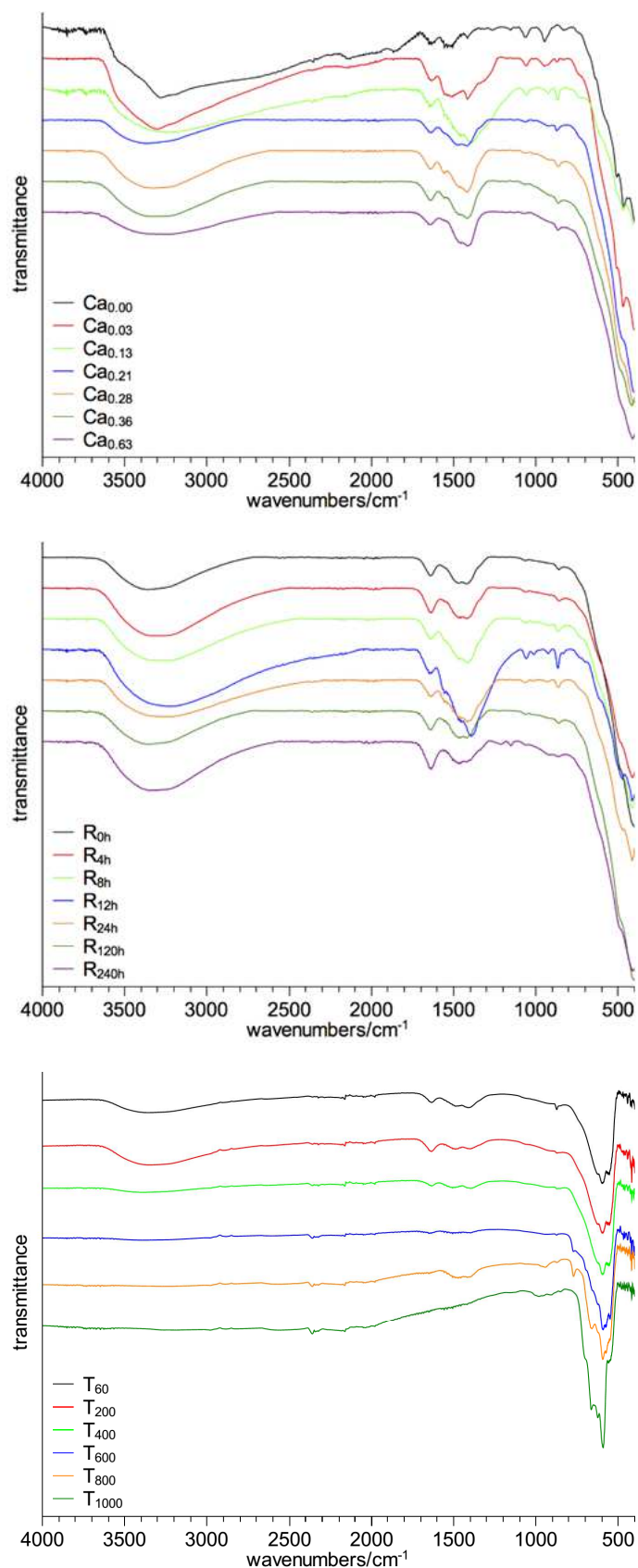


**Figure S3.** ATR-IR spectra of powder samples of the studied synthetic oxides. From top to bottom, the spectra for the Ca<sub>□</sub>, R<sub>y</sub> and T<sub>z</sub> series of oxides are shown.

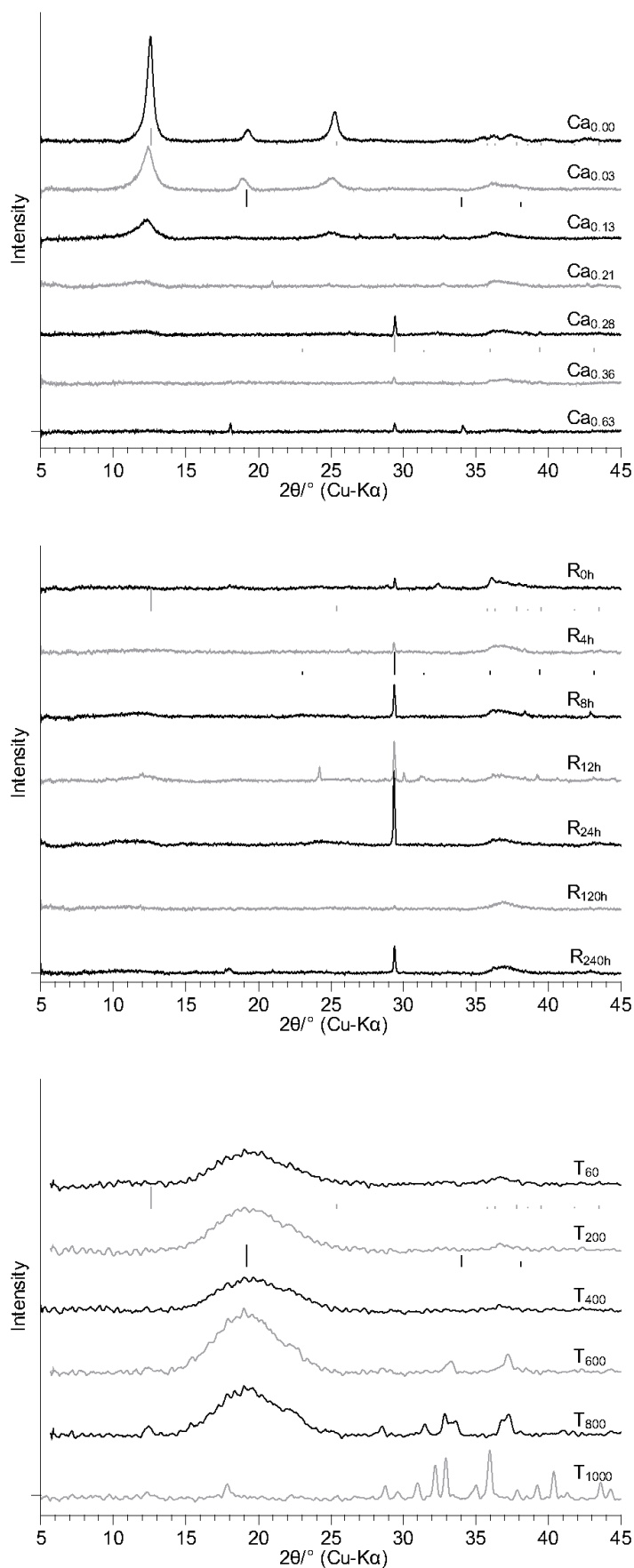


**Figure S4.** Powder XRD patterns for the oxides of the  $\text{Ca}_x$ ,  $\text{R}_y$  and  $\text{T}_z$  series. The theoretical patterns for birnessite (below  $\text{Ca}_{0.00}$ ,  $\text{R}_{0\text{h}}$  and  $\text{T}_{60}$  in grey), feitknechtite ( $\beta\text{-MnO}(\text{OH})$ , below  $\text{Ca}_{0.03}$  and  $\text{T}_{200}$  in black) and  $\text{CaCO}_3$  impurities (below  $\text{Ca}_{0.28}$  and  $\text{R}_{4\text{h}}$ ) are also shown. The broad reflections centred at around  $2\theta = \sim 29^\circ$  visible for the  $\text{T}_z$  series originate from the polyacetate films used to hold the powder samples in position.

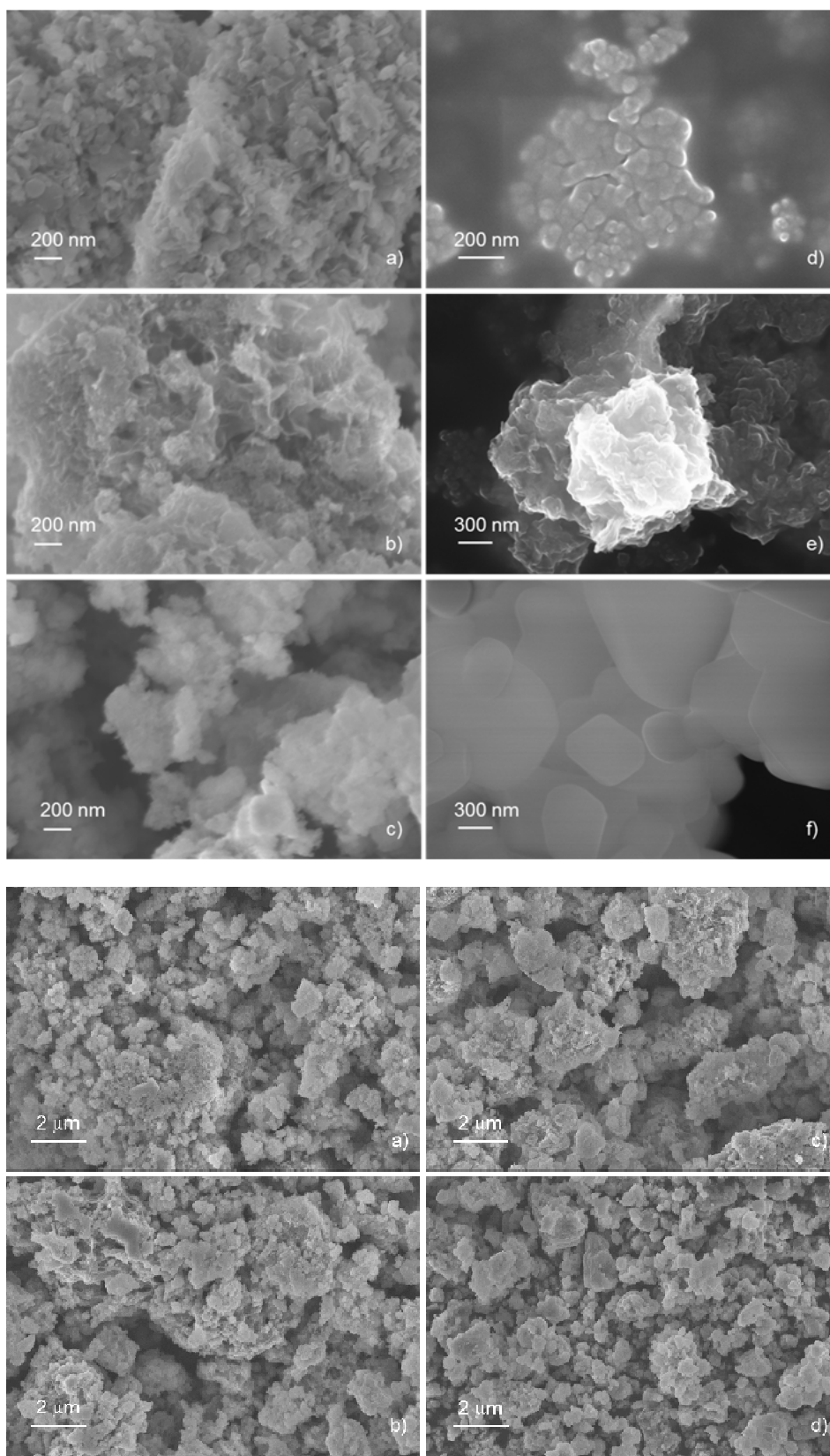


**Figure S5.** *top*: SEM images of the oxides  $\text{Ca}_{0.00}$ ,  $\text{Ca}_{0.21}$  and  $\text{Ca}_{0.63}$  from the calcium series (a - c) as well as  $\text{T}_{60}$ ,  $\text{T}_{400}$  and  $\text{T}_{1000}$  from the temperature series (d-f) at higher resolution (magnification: a-c) 100 000x, d) 200 000x e)-f) 100 000x); *bottom*: micrographs of the oxides  $\text{R}_{0h}$ ,  $\text{R}_{8h}$ ,  $\text{R}_{24h}$  and  $\text{R}_{240h}$  (magnification: 20 000x).

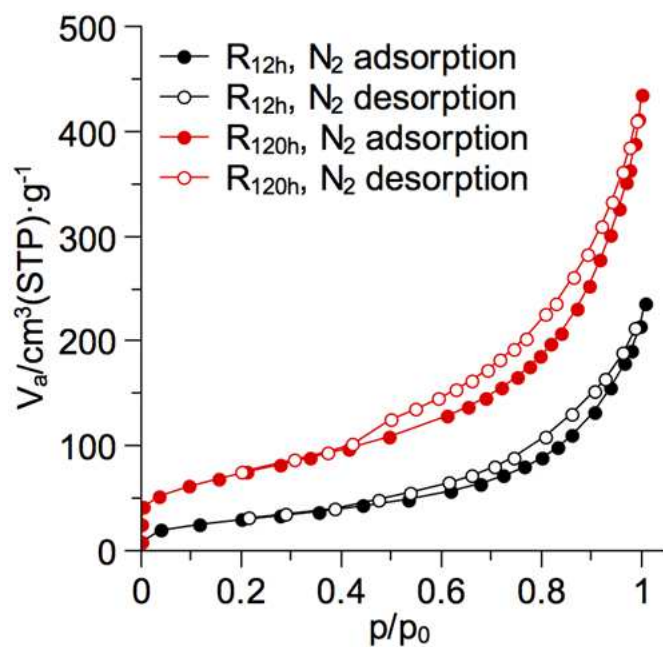


**Figure S6.**  $\text{N}_2$  adsorption/desorption isotherms for two oxides of the  $R_y$  series. The isotherms were recorded at 77 K after activation of the oxide samples at 120 °C for 2 h.

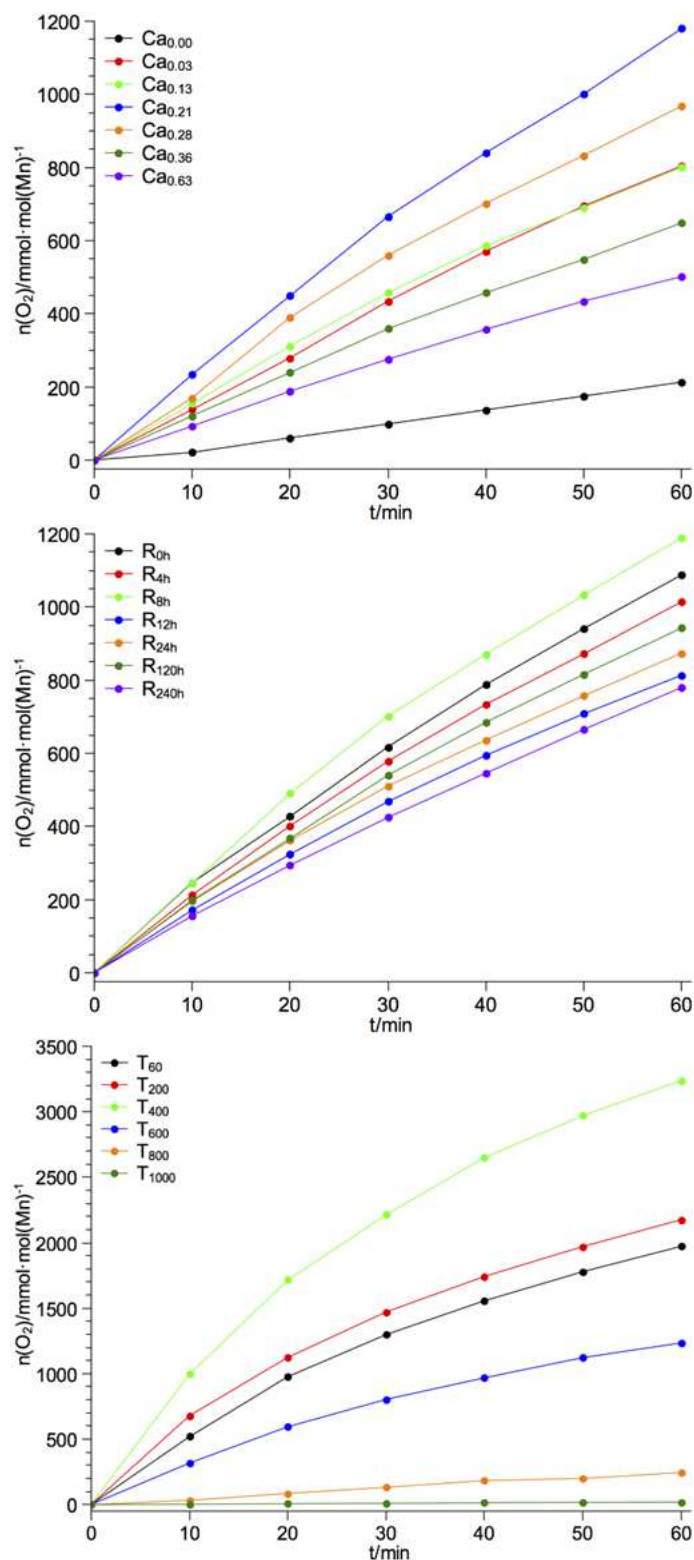


**Figure S7.** Representative oxygen evolution curves for reactions of oxides from the  $\text{Ca}_x$ ,  $\text{R}_y$  and  $\text{T}_z$  series with  $\text{Ce}^{4+}$  solutions at  $40^\circ\text{C}$ .

## References

- 1 G. Jander, K. F. Jahr, G. Schulze and J. Simon, *Maßanalyse. Theorie und Praxis der Titrationsen mit chemischen und physikalischen Indikationen*, de Gruyter, Berlin, 16th edn., 2003.
- 2 M. Wiechen, I. Zaharieva, H. Dau and P. Kurz, *Chem. Sci.*, 2012, **3**, 2330–2339.
- 3 a) A. Iyer, J. Del-Pilar, C. K. King'ondou, E. Kissel, H. F. Garces, H. Huang, A. M. El-Sawy, P. K. Dutta and S. L. Suib., *J. Phys. Chem. C*, 2012, **116**, 6474–6483; b) M. M. Najafpour, D. J. Sedigh, B. Pashaei and S. Nayeri, *New J. Chem.*, 2013, **37**, 2448.
- 4 D. M. Robinson, Y. B. Go, M. Mui, G. Gardner, Z. Zhang, D. Mastrogiovanni, E. Garfunkel, J. Li, M. Greenblatt and G. C. Dismukes, *J. Am. Chem. Soc.*, 2013, **135**, 3494–3501.